JOURNAL OF GUIDANCE, CONTROL, AND DYNAMICS
Vol. 45, No. 11, November 2022

Check for updates

Engineering Notes

Nonlinear Guidance Law for Target Enclosing with Arbitrary Smooth Shapes

Abhinav Sinha* and Yongcan Cao†
The University of Texas at San Antonio, San Antonio, Texas 78249

https://doi.org/10.2514/1.G006957

Downloaded by "University of Texas, San Antonio" on June 15, 2025 | http://arc.aiaa.org | DOI: 10.2514/1.G006957

I. Introduction

WITH requirements for increased autonomy, unmanned aerial vehicles (UAVs) have become prominent in applications such as area coverage and observation, surveillance, environmental monitoring, aerial defense, reconnaissance, and search and rescue. A majority of these applications require that a pursuing unmanned vehicle, referred to as the *pursuer*, maintains a certain geometrical shape/pattern/trajectory around another vehicle or a beacon or any point of interest, called the *target*. Maintaining the desired pattern around a target is referred to as target enclosing, and has many promising civilian and military applications.

One of the pioneering works in target enclosing using mobile robotic troops was studied in the work of Yamaguchi [1], where the vehicles were assumed to satisfy holonomic dynamics. Similar studies on holonomic vehicle dynamics for target enclosing were also reported in Refs. [2,3]. While considering vehicles with holonomic dynamics may simplify the control design, the consideration of nonholonomic vehicle dynamics is much more challenging and practical, and has been studied in, e.g., [4–6], for target enclosing as a formation control problem. Among many different formation tasks, orbiting a target in a circle (also known as *target encirclement* or *standoff tracking* or *circumnavigation*) has received significant attention [7–25].

One of the approaches in this direction utilizes the concept of vector fields surrounding the desired path or a geometrical pattern to manipulate the vehicle's heading onto it. In Ref. [9], the authors constructed a Lyapunov vector field to circumnavigate a stationary target on different altitudes using multiple UAVs, while a coordinated standoff tracking in the presence of wind was presented in Ref. [10]. Lim et al. [11] designed vector fields producing stable convergence to a limit cycle of the desired radius around the target, thereby enabling the vehicles to circumnavigate the target with a fixed radius. A guidance law for curvature-constrained standoff tracking using Lyapunov vector fields was presented in Ref. [12]. To improve the convergence time to the standoff circle as compared to that using vector fields, Quigley et al. [13] used Hopf bifurcation. In Ref. [14], a tangent-plus-Lyapunov vector field was used by including a switching logic between tangent and Lyapunov vector fields to improve the convergence to the standoff circle further. A nonlinear model predictive control was presented in Ref. [15] for coordinated standoff tracking by a pair of vehicles to achieve optimal performance. Yoon et al. [16] relied on spherical pendulum motion to design a standoff tracking guidance law by regulating the position and velocity errors using backstepping and Lyapunov stability.

In the existing literature, several other strategies devised their guidance laws using only relative range [17–20], only the pursuer's look angle [21,22], or both relative range and the pursuer's look angle [23]. In Ref. [17], an adaptive localization algorithm was presented for slow drifting targets. A sliding mode controller was designed in Ref. [18] for wheeled mobile robots to circumnavigate a target. In Ref. [19], a geometric approach was put forth to drive the pursuer toward a tangent point of an auxiliary circle. Recently, Dong et al. [20] presented a backstepping-based target enclosing guidance law with any desired smooth pattern. However, the guidance law in Ref. [20] was limited to enclosing stationary targets. Using the pursuer's look angle only, localization and circumnavigation of a slowly moving target with unknown speed were addressed in Ref. [21], while enclosing both point and disk targets was considered in Ref. [22]. Using noise in both relative range and look angle measurements, the strategy in Ref. [23] proposed a circumnavigating controller that can also control the direction of encirclement. By controlling the vehicle's side-bearing angle, the work in Refs. [24,25] presented an asymptotic guidance law for target enclosing.

It is worth noting that most of the existing strategies are concerned with target encirclement only. However, such an enclosing may not suffice in complicated environments or scenarios involving boundary tracking, perimeter surveillance, herding/shepherding, enclosing multiple targets, covert missions, etc., because the pursuer may have to deviate from a circular orbit occasionally. Moreover, most existing designs focused on circumnavigating a stationary target, resulting in limited use cases. Some have extended their techniques to enclose a constant-speed target. However, most of the existing designs cannot be directly extended for enclosing a general maneuvering target. Hence, it is more pragmatic to design a guidance law that is capable of enclosing a mobile target with more geometrical patterns instead of a circle. It is often expected in practice that the target enclosing requirements be satisfied as early as possible. Specifically, making the pursuer converge to the desired geometrical shape within finite time may have advantages in terms of better guidance precision and disturbance attenuation. This requirement serves as another motivation for the proposed work where we can exercise control over the transient phase directly through the guidance command. Thus, in light of the aforementioned works, we now summarize the main contributions of our paper below:

1) We propose a novel guidance strategy that allows a pursuer to enclose a target within any desired reference (smooth and bounded) geometrical shape/pattern. Enclosing a target within a geometrical shape/pattern other than a circle allows for more area coverage, and may provide potential benefits in complicated environments.

2) The proposed strategy does not require the target's guidance law or the information about its maneuver sequence, given that such information is usually difficult to obtain. This makes the proposed design fairly simple and independent of the target's maneuver.

3) In practice, a vehicle cannot instantaneously turn on a dime. Instead of directly manipulating the vehicle's heading or turn rate (as done in most existing studies), our consideration of the pursuer's lateral acceleration as its steering control makes the design more accurate and well-suited for aerial vehicles.

4) The proposed control design approach uses predefined-time convergent sliding mode control [26] to shorten the transient phase by directly specifying the upper bound of the settling time in the guidance command, thus enabling the pursuer to converge to the desired geometrical shape quickly.

Received 12 May 2022; revision received 6 July 2022; accepted for publication 6 July 2022; published online 22 July 2022. Copyright © 2022 by Abhinav Sinha and Yongcan Cao. Published by the American Institute of Aeronautics and Astronautics, Inc., with permission. All requests for copying and permission to reprint should be submitted to CCC at www.copyright.com; employ the eISSN 1533-3884 to initiate your request. See also AIAA Rights and Permissions www.aiaa.org/randp.

*Postdoctoral Fellow, Unmanned Systems Laboratory, Department of Electrical and Computer Engineering; abhinav.sinha@utsa.edu.

†Associate Professor, Unmanned Systems Laboratory; yongcan.cao@utsa.edu.

Downloaded by "University of Texas, San Antonio" on June 15, 2025 | http://arc.aiaa.org | DOI: 10.2514/1.G006957

The remainder of this paper is organized as follows. In Sec. II, we present the kinematics of pursuer–target engagement, followed by the problem statement. We formally derive the proposed guidance strategy for the pursuer in Sec. III, followed by Sec. IV, wherein we demonstrate various scenarios attesting the efficacy and applicability of the proposed method. In Sec. V, we conclude our paper and provide outlines toward future investigations.

II. Problem Formulation

Consider a scenario where a pursuer aims to enclose a target within a given geometrical shape, as shown in Fig. 1a. In this scenario, the target may be a ground station, a beacon, or an area of interest to be monitored, or it can be another vehicle. Figure 1b depicts the engagement geometry for such a scenario. The pursuer, whose speed and flight path angle are denoted by v_{M} and γ_{M}, respectively, is steered by the lateral acceleration a_{M} applied perpendicular to its velocity. The relative line-of-sight (LOS) separation, or the relative range, between the pursuer and the target, is denoted by r, while θ represents the LOS angle. The pursuer's look angle, which is the angle between its heading and the LOS, is σ. Without loss of generality, we assume that the target is mobile and exhibits similar characteristics as that of the pursuer; i.e., for the target whose speed is v_{T}, the steering control a_{T} is its lateral acceleration applied normal to its velocity. The target's flight path angle is denoted by γ_{T}.

We assume the vehicles to be point mass objects, whose speeds remain invariant throughout the engagement. However, the pursuer has a speed advantage over the target; i.e., $v_{\mathrm{M}} > v_{\mathrm{T}}$. It is also reasonable to assume that the inner control loop is quite faster than the outer guidance loop; thus we neglect the dynamics of the autopilot while deriving the guidance command for target enclosing. The following set of equations describes the relative motion for the pursuer–target engagement, in polar coordinates:

$$v_r = \dot{r} = v_{\mathrm{T}}\cos(\gamma_{\mathrm{T}} - \theta) - v_{\mathrm{M}}\cos\sigma \tag{1a}$$

$$v_\theta = r\dot{\theta} = v_{\mathrm{T}}\sin(\gamma_{\mathrm{T}} - \theta) - v_{\mathrm{M}}\sin\sigma \tag{1b}$$

$$\sigma = \gamma_{\mathrm{M}} - \theta \tag{1c}$$

where v_r and v_θ are the relative velocity components along and across the LOS. We further assume that the lateral acceleration of the ith vehicle is bounded such that

$$\dot{\gamma}_i = \frac{a_i}{v_i};\ |a_i| \le a_i^{\max}, \quad \forall i \in \{\mathrm{M}, \mathrm{T}\} \tag{2}$$

Note that we choose the vehicle's lateral acceleration as its steering control because most aerial vehicles require the necessary lift to fly, which manipulates the vehicle's lateral acceleration to steer it on the requisite course [27–32]. Considering acceleration as the steering control also means that the vehicles are turn-constrained; i.e., they cannot turn on a dime but have a turning radius. This consideration also brings the design closer to practice.

The goal of this paper is to design a nonlinear guidance strategy for the pursuer to enclose the target within a given geometrical shape. While encirclement, or maintaining a standoff distance from the target, is the most common enclosing encountered in the literature, the proposed guidance strategy subsumes encirclement guidance as a special case, as will be shown in the sequel.

It is also desirable that the strategy so designed allows global convergence to the desired enclosing geometry; i.e., the pursuer should be able to enclose the target even if it is initially far away from the desired enclosing geometry. Our consideration of this problem in a nonlinear framework also circumvents the errors associated with linear approximations.

III. Main Results

In this section, we derive the guidance command for the pursuer to enclose a mobile target within an arbitrary smooth and bounded geometrical shape using relative measurements. Note that target enclosing essentially means that the pursuer remains at a certain nonzero distance from the target; however, this distance may not be a constant value. This observation leads to speculation that any given geometrical shape around the target can be instantaneously specified using the desired relative distance between the pursuer and the target.

Let us denote the desired time-varying relative range between the pursuer and the target by $r_{\mathrm{d}}(t)$, which serves as a parameter for target enclosing. It is also worth noting that $r_{\mathrm{d}}(t)$ should be smooth and bounded for any enclosing to be meaningful. The reasons for this requirement will become obvious in the sequel. Thus, the problem of enclosing a target within a given geometrical shape translates to that of controlling the relative range between the vehicles.

Consider the error variable

$$\epsilon = r - r_{\mathrm{d}} \tag{3}$$

where we have dropped the argument denoting the time dependency of r_{d} for brevity. However, v_r as in Eq. (1a) is also important to consider from the pursuer's viewpoint because it dictates whether the pursuer is heading toward the enclosing geometry or away from it.

Lemma 1: The dynamics of the error, Eq. (3), has a relative degree two with respect to the pursuer's lateral acceleration.

Proof: Subsequent differentiation of Eq. (3) with respect to time, and using Eq. (1), results in

$$\begin{aligned}\dot{\epsilon} &= \dot{r} - \dot{r}_{\mathrm{d}} = v_{\mathrm{T}}\cos(\gamma_{\mathrm{T}} - \theta) - v_{\mathrm{M}}\cos\sigma - \dot{r}_{\mathrm{d}} \\ \Rightarrow \ddot{\epsilon} &= \ddot{r} - \ddot{r}_{\mathrm{d}} = -v_{\mathrm{T}}\sin(\gamma_{\mathrm{T}} - \theta)\left(\dot{\gamma}_{\mathrm{T}} - \dot{\theta}\right) + v_{\mathrm{M}}\sin\sigma\left(\dot{\gamma}_{\mathrm{M}} - \dot{\theta}\right) - \ddot{r}_{\mathrm{d}}\end{aligned} \tag{4}$$

since $\dot{\sigma} = \dot{\gamma}_{\mathrm{M}} - \dot{\theta}$. The expression in Eq. (4) can be further simplified using Eq. (2) as

$$\begin{aligned}\ddot{\epsilon} &= -v_{\mathrm{T}}\sin(\gamma_{\mathrm{T}} - \theta)\left(\frac{a_{\mathrm{T}}}{v_{\mathrm{T}}} - \dot{\theta}\right) + v_{\mathrm{M}}\sin\sigma\left(\frac{a_{\mathrm{M}}}{v_{\mathrm{M}}} - \dot{\theta}\right) - \ddot{r}_{\mathrm{d}} \\ &= (v_{\mathrm{T}}\sin(\gamma_{\mathrm{T}} - \theta) - v_{\mathrm{M}}\sin\sigma)\dot{\theta} + a_{\mathrm{M}}\sin\sigma - a_{\mathrm{T}}\sin(\gamma_{\mathrm{T}} - \theta) - \ddot{r}_{\mathrm{d}}\end{aligned} \tag{5}$$

which can be expressed, using Eq. (1b), as

$$\ddot{\epsilon} = r\dot{\theta}^2 + a_{\mathrm{M}}\sin\sigma - a_{\mathrm{T}}\sin(\gamma_{\mathrm{T}} - \theta) - \ddot{r}_{\mathrm{d}} \tag{6}$$

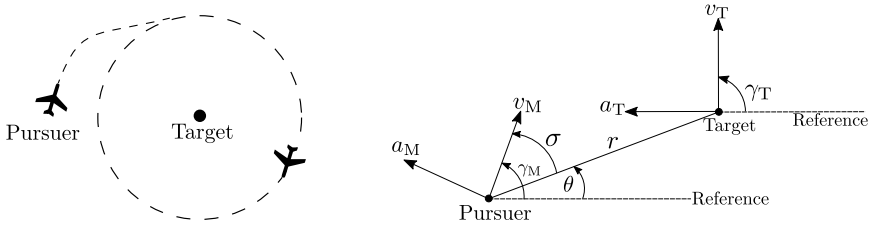

a) Target enclosing within a circle **b) Planar engagement geometry**

Fig. 1 Pursuer–target engagement geometry for target enclosing.

From Eq. (6), we observe that the lateral accelerations of both the vehicles appear in the second derivative of ϵ. This concludes the proof. □

We also observe from Lemma 1 that the expression in Eq. (6) also contains $\ddot{r}_\mathrm{d}$. Thus, it is apparent that a valid r_d should be smooth, bounded, and at least $\mathbb{C}^2$. For all intents and purposes, this is a reasonable assumption because an unbounded desired relative range does not actually correspond to enclosing in practice. Thus, it is assumed that

$$r_\mathrm{d}^{\min} \le r_\mathrm{d} \le r_\mathrm{d}^{\max}, \quad |\dot{r}_\mathrm{d}| \le \dot{r}_\mathrm{d}^{\max} < \infty, \quad |\ddot{r}_\mathrm{d}| \le \ddot{r}_\mathrm{d}^{\max} < \infty \tag{7}$$

Further, we also note the presence of the target's maneuver in Eq. (6), and that accounting for the target's motion while enclosing it is challenging. Although the necessary engagement variables can be measured or estimated with certain accuracy, having knowledge of the target's strategy is usually difficult. However, the target's maneuver sequence may be either estimated or can be treated as a bounded uncertainty in the design. In this paper, we consider it as a bounded uncertainty because its upper bound may be known. Consequently, the need for an additional estimator is eliminated, and the proposed design becomes simpler.

From Eq. (3) and the results in Lemma 1, we infer that we seek a guidance strategy that can drive ϵ and $\dot{\epsilon}$ to zero, preferably within a time whose upper bound can be specified through the guidance command. This essentially means that the proposed strategy should be capable of shortening the transient phase at will, leading to advantages such as disturbance attenuation and better precision of the guidance command. To this aim, we design the proposed strategy using a predefined-time convergent sliding mode control [26], which is known to provide insensitivity to such anomalies, and has been applied to other guidance problems where time of convergence is crucial [27]. Hence, we consider a sliding manifold of the form

$$\mathcal{S} = \epsilon + \beta \dot{\epsilon}^{\frac{p}{q}}; \ \beta > 0 \tag{8}$$

where p and q are odd integers such that $p > q$ and $1 < p/q < 2$. Before presenting the main result of this paper, we recall an important result regarding the predefined-time stability of a nonlinear system.

Lemma 2 ([26]): For a nonlinear system $\dot{z} = f(z)$ with $f(0) = 0$, if there exists a continuous and radially unbounded positive definite function $\mathcal{V}(z)$ for some $\mathcal{M}$, $\mathcal{N}$, m, n, $k > 0$ that satisfy $mk < 1$, $nk > 1$, such that

$$\dot{\mathcal{V}}(z) \le -\frac{\Gamma\left(\frac{1-mk}{n-m}\right)\Gamma\left(\frac{nk-1}{n-m}\right)}{\mathcal{M}^k\Gamma(k)(n-m)T_s}\left(\frac{\mathcal{M}}{\mathcal{N}}\right)^{\frac{1-mk}{n-m}}\left(\mathcal{M}\mathcal{V}^m(z) + \mathcal{N}\mathcal{V}^n(z)\right)^k \tag{9}$$

where $T_s > 0$ is the least upper bound on the settling time, and $\Gamma(\cdot):\Gamma(w) = \int_0^\infty e^{-y}y^{w-1}\,\mathrm{d}y$ for all $w \in \boldsymbol{C}$ is the gamma function with the real part of w being positive, namely, $\Re\{w\} > 0$, then the origin of the nonlinear system is stable in a predefined time T_s.

We are now equipped to present the main result of this paper, whose essence is given by the following theorem.

Theorem 1: Consider the planar engagement between a pursuer and a target whose kinematics is governed by Eq. (1), and the error variable, Eq. (3). The pursuer's lateral acceleration

$$a_\mathrm{M} = -\frac{\left(\frac{\Gamma\left(\frac{1-mk}{n-m}\right)\Gamma\left(\frac{nk-1}{n-m}\right)}{\mathcal{M}^k\Gamma(k)(n-m)T_s}\left(\frac{\mathcal{M}}{\mathcal{N}}\right)^{\frac{1-mk}{n-m}}\left(\mathcal{M}|\mathcal{S}|^m + \mathcal{N}|\mathcal{S}|^n\right)^k + \eta\right)\mathrm{sign}(\mathcal{S}) + (v_\mathrm{T}\cos(\gamma_\mathrm{T}-\theta) - v_\mathrm{M}\cos\sigma - \dot{r}_\mathrm{d})}{\beta\frac{p}{q}\left(v_\mathrm{T}\cos(\gamma_\mathrm{T}-\theta) - v_\mathrm{M}\cos\sigma - \dot{r}_\mathrm{d}\right)^{\frac{p}{q}-1}\sin\sigma} + \frac{r\ddot{r}_\mathrm{d} - (v_\mathrm{T}\sin(\gamma_\mathrm{T}-\theta) - v_\mathrm{M}\sin\sigma)^2}{r\sin\sigma} \tag{10}$$

where

$$\eta > \frac{\beta p}{q}\left(v_\mathrm{T} + v_\mathrm{M} + \dot{r}_\mathrm{d}^{\max}\right)^{\frac{p}{q}-1}a_\mathrm{T}^{\max} \tag{11}$$

and $\mathcal{M}$, $\mathcal{N}$, m, n, k satisfy the conditions in Lemma 2, allows the pursuer to converge to the desired target enclosing geometry within finite time $T_s + t_c$, where T_s is the upper bound on the time of occurrence of sliding mode on the chosen sliding manifold, Eq. (8), which can be directly specified through Eq. (10), and

$$t_c = \frac{p}{p-q}|\epsilon(T_s)|^{1-\frac{q}{p}} \tag{12}$$

Proof: By considering a Lyapunov function candidate $\mathcal{V} = |\mathcal{S}|$, and differentiating it and Eq. (8) with respect to time, we obtain

$$\dot{\mathcal{V}} = \dot{\mathcal{S}}\mathrm{sign}(\mathcal{S}) = \left[\dot{\epsilon} + \frac{\beta p}{q}\dot{\epsilon}^{\frac{p}{q}-1}\ddot{\epsilon}\right]\mathrm{sign}(\mathcal{S}) \tag{13}$$

which can be simplified using the results in Lemma 1 as

$$\begin{aligned}\dot{\mathcal{V}} &= \left[\dot{\epsilon} + \frac{\beta p}{q}\dot{\epsilon}^{\frac{p}{q}-1}\ddot{\epsilon}\right]\mathrm{sign}(\mathcal{S})\\ &= \left[\dot{r} - \dot{r}_\mathrm{d} + \frac{\beta p}{q}(\dot{r} - \dot{r}_\mathrm{d})^{\frac{p}{q}-1}(r\dot{\theta}^2 + a_\mathrm{M}\sin\sigma\right.\\ &\quad \left. - a_\mathrm{T}\sin(\gamma_\mathrm{T}-\theta) - \ddot{r}_\mathrm{d})\right]\mathrm{sign}(\mathcal{S})\end{aligned}$$

Substituting Eq. (1a) in the above expression yields

$$\begin{aligned}\dot{\mathcal{V}} = \Bigg[&v_\mathrm{T}\cos(\gamma_\mathrm{T}-\theta) - v_\mathrm{M}\cos\sigma - \dot{r}_\mathrm{d}\\ &+ \frac{\beta p}{q}\left(v_\mathrm{T}\cos(\gamma_\mathrm{T}-\theta) - v_\mathrm{M}\cos\sigma - \dot{r}_\mathrm{d}\right)^{\frac{p}{q}-1}\\ &\times\left(r\dot{\theta}^2 + a_\mathrm{M}\sin\sigma - a_\mathrm{T}\sin(\gamma_\mathrm{T}-\theta) - \ddot{r}_\mathrm{d}\right)\Bigg]\mathrm{sign}(\mathcal{S}).\end{aligned}$$

If we choose the pursuer's lateral acceleration as the one given in Eq. (10), then $\dot{V}$, given above, reduces to

$$\begin{aligned}\dot{\mathcal{V}} &= \Bigg[-\left(\Upsilon(\mathcal{M}|\mathcal{S}|^m + \mathcal{N}|\mathcal{S}|^n)^k + \eta\right)\mathrm{sign}(\mathcal{S})\\ &\quad -\frac{\beta p}{q}\left(v_\mathrm{T}\cos(\gamma_\mathrm{T}-\theta) - v_\mathrm{M}\cos\sigma - \dot{r}_\mathrm{d}\right)^{\frac{p}{q}-1}a_\mathrm{T}\sin(\gamma_\mathrm{T}-\theta)\Bigg]\mathrm{sign}(\mathcal{S})\\ &\le -\left(\Upsilon(\mathcal{M}|\mathcal{S}|^m + \mathcal{N}|\mathcal{S}|^n)^k + \eta\right)\\ &\quad -\frac{\beta p}{q}\left(v_\mathrm{T}\cos(\gamma_\mathrm{T}-\theta) - v_\mathrm{M}\cos\sigma - \dot{r}_\mathrm{d}\right)^{\frac{p}{q}-1}a_\mathrm{T}\sin(\gamma_\mathrm{T}-\theta)\mathrm{sign}(\mathcal{S})\\ &\le -\Upsilon\left(\mathcal{M}|\mathcal{S}|^m + \mathcal{N}|\mathcal{S}|^n\right)^k\\ &\quad -\left(\eta - \frac{\beta p}{q}\left(v_\mathrm{T}\cos(\gamma_\mathrm{T}-\theta) - v_\mathrm{M}\cos\sigma - \dot{r}_\mathrm{d}\right)^{\frac{p}{q}-1}a_\mathrm{T}^{\max}\right)\\ &\le -\Upsilon\left(\mathcal{M}|\mathcal{S}|^m + \mathcal{N}|\mathcal{S}|^n\right)^k - \left(\eta - \frac{\beta p}{q}\left(v_\mathrm{T} + v_\mathrm{M} + \dot{r}_\mathrm{d}^{\max}\right)^{\frac{p}{q}-1}a_\mathrm{T}^{\max}\right)\end{aligned} \tag{14}$$

Downloaded by "University of Texas, San Antonio" on June 15, 2025 | http://arc.aiaa.org | DOI: 10.2514/1.G006957

where

$$\Upsilon = \frac{\Gamma\left(\frac{1-mk}{n-m}\right)\Gamma\left(\frac{nk-1}{n-m}\right)}{\mathcal{M}^k\Gamma(k)(n-m)T_s}\left(\frac{\mathcal{M}}{\mathcal{N}}\right)^{\frac{1-mk}{n-m}} \tag{15}$$

If η satisfies Eq. (11), then Eq. (14) becomes

$$\begin{aligned}\dot{\mathcal{V}} &\leq -\frac{\Gamma\left(\frac{1-mk}{n-m}\right)\Gamma\left(\frac{nk-1}{n-m}\right)}{\mathcal{M}^k\Gamma(k)(n-m)T_s}\left(\frac{\mathcal{M}}{\mathcal{N}}\right)^{\frac{1-mk}{n-m}}(\mathcal{M}|\mathcal{S}|^m + \mathcal{N}|\mathcal{S}|^n)^k \\ &= -\frac{\Gamma\left(\frac{1-mk}{n-m}\right)\Gamma\left(\frac{nk-1}{n-m}\right)}{\mathcal{M}^k\Gamma(k)(n-m)T_s}\left(\frac{\mathcal{M}}{\mathcal{N}}\right)^{\frac{1-mk}{n-m}}(\mathcal{M}\mathcal{V}^m + \mathcal{N}\mathcal{V}^n)^k < 0,\ \forall \mathcal{V} \neq 0\end{aligned} \tag{16}$$

which, according to the results in Lemma 2, implies that $\mathcal{V}$ goes to 0 within a predefined time T_s independent of its initial value. Consequently, $\mathcal{S}$ becomes 0 within a predefined time T_s.

Because the reaching phase can be shortened by specifying an arbitrarily small T_s, it follows that after sliding mode is enforced, the errors ϵ and $\dot{\epsilon}$ vanish within t_c, as given in Eq. (12). This essentially implies that the pursuer converges to the desired enclosing geometry around the target within finite time $T_s + t_c$. This concludes the proof. □

Note that Eq. (11) only gives a sufficient condition on η. If we express Eq. (10) in an alternate form as

$$a_{\mathrm{M}} = -\frac{q(v_r - \dot{r}_{\mathrm{d}})^{1-\frac{p}{q}}\left[\left(\frac{\Gamma\left(\frac{1-mk}{n-m}\right)\Gamma\left(\frac{nk-1}{n-m}\right)}{\mathcal{M}^k\Gamma(k)(n-m)T_s}\left(\frac{\mathcal{M}}{\mathcal{N}}\right)^{\frac{1-mk}{n-m}}(\mathcal{M}|\mathcal{S}|^m + \mathcal{N}|\mathcal{S}|^n)^k + \eta\right)\mathrm{sign}(\mathcal{S}) + (v_r - \dot{r}_{\mathrm{d}})\right]}{\beta p \sin\sigma} + \frac{r\ddot{r}_{\mathrm{d}} - v_\theta^2}{r\sin\sigma} \tag{17}$$

then it follows that the proposed guidance command contains information about relative measurements only. It is also worth noting that the target's strategy or even its maneuver sequence is not required for the pursuer to enclose it. In this paper, we assume that the target's speed is known. However, it can be computed using relative measurements as

$$v_{\mathrm{T}} = \sqrt{(v_r + v_{\mathrm{M}}\cos\sigma)^2 + (v_\theta + v_{\mathrm{M}}\sin\sigma)^2} \tag{18}$$

Once v_{T} is known, one can simply compute the target's heading angle as

$$\begin{aligned}\gamma_{\mathrm{T}} &= \theta + \cos^{-1}\left(\frac{v_r + v_{\mathrm{M}}\cos\sigma}{v_{\mathrm{T}}}\right) \\ &= \theta + \sin^{-1}\left(\frac{v_\theta + v_{\mathrm{M}}\sin\sigma}{v_{\mathrm{T}}}\right)\end{aligned}$$

In our work, however, we do not require information about the target's mobility to design the pursuer's guidance law. The proposed guidance law is effective even without the information about the target's maneuver/strategy, which also avoids heavy computations and prevents the design from being complicated.

From the expression of a_{M} in Theorem 1, one may observe that the look angle σ appears in the denominator. Despite that, the guidance command is nonsingular. An analysis of the behavior of the pursuer's look angle confirms the above claim. From Lemma 2, it follows that T_s can be chosen sufficiently small to reduce the transient phase. In fact, one of the motivations to use a predefined-time convergent sliding mode control is to shorten the transient phase at will by specifying the upper bound of the settling time (as a design parameter) directly in the guidance command. If the settling time is chosen sufficiently small, then the look angle may not have a chance to become zero in most cases. If at the beginning of the engagement, $\sigma(0) = 0$, then even with a minuscule perturbation in the pursuer's heading angle, γ_{M} can make $\sigma \neq 0$, thus reducing the chance of a singularity in the initial or transient engagement phase. Therefore, it is more meaningful to analyze the behavior of σ once the sliding mode is enforced on $\mathcal{S}$, which is the essence of the next theorem.

Theorem 2: The pursuer's look angle σ is nonzero almost everywhere during target enclosing, which implies that the proposed guidance command, Eq. (10), is nonsingular almost everywhere.

Proof: To prove that the pursuer's look angle does not become zero, it is equivalent to prove that $\sigma = 0$ is not an equilibrium point of the system $\dot{\sigma} = f(\sigma)$ in the interval $(-\pi, \pi)$. Hence, we proceed as follows:

Differentiating Eq. (1c) with respect to time and using Eqs. (1) and (2) yield

$$\begin{aligned}\dot{\sigma} &= \dot{\gamma}_{\mathrm{M}} - \dot{\theta} \\ &= \frac{a_{\mathrm{M}}}{v_{\mathrm{M}}} - \frac{v_{\mathrm{T}}\sin(\gamma_{\mathrm{T}} - \theta) - v_{\mathrm{M}}\sin\sigma}{r}\end{aligned} \tag{19}$$

which can be further simplified, by substituting the steady-state value of Eq. (10), as

$$\begin{aligned}\dot{\sigma} &= -\frac{(v_{\mathrm{T}}\cos(\gamma_{\mathrm{T}} - \theta) - v_{\mathrm{M}}\cos\sigma - \dot{r}_{\mathrm{d}})}{\beta\frac{p}{q}(v_{\mathrm{T}}\cos(\gamma_{\mathrm{T}} - \theta) - v_{\mathrm{M}}\cos\sigma - \dot{r}_{\mathrm{d}})^{\frac{p}{q}-1}v_{\mathrm{M}}\sin\sigma} \\ &\quad + \frac{r\ddot{r}_{\mathrm{d}} - (v_{\mathrm{T}}\sin(\gamma_{\mathrm{T}} - \theta) - v_{\mathrm{M}}\sin\sigma)^2}{rv_{\mathrm{M}}\sin\sigma} - \frac{v_{\mathrm{T}}\sin(\gamma_{\mathrm{T}} - \theta) - v_{\mathrm{M}}\sin\sigma}{r} \\ &= -\frac{(v_{\mathrm{T}}\cos(\gamma_{\mathrm{T}} - \theta) - v_{\mathrm{M}}\cos\sigma - \dot{r}_{\mathrm{d}})}{\beta\frac{p}{q}(v_{\mathrm{T}}\cos(\gamma_{\mathrm{T}} - \theta) - v_{\mathrm{M}}\cos\sigma - \dot{r}_{\mathrm{d}})^{\frac{p}{q}-1}v_{\mathrm{M}}\sin\sigma} + \frac{\ddot{r}_{\mathrm{d}}}{v_{\mathrm{M}}\sin\sigma} \\ &\quad - \frac{(v_{\mathrm{T}}\sin(\gamma_{\mathrm{T}} - \theta) - v_{\mathrm{M}}\sin\sigma)^2}{rv_{\mathrm{M}}\sin\sigma} - \frac{(v_{\mathrm{T}}\sin(\gamma_{\mathrm{T}} - \theta) - v_{\mathrm{M}}\sin\sigma)}{r} \\ &= -\frac{(v_{\mathrm{T}}\cos(\gamma_{\mathrm{T}} - \theta) - v_{\mathrm{M}}\cos\sigma - \dot{r}_{\mathrm{d}})^{2-\frac{p}{q}}}{\beta\frac{p}{q}v_{\mathrm{M}}\sin\sigma} + \frac{\ddot{r}_{\mathrm{d}}}{v_{\mathrm{M}}\sin\sigma} \\ &\quad - \frac{(v_{\mathrm{T}}\sin(\gamma_{\mathrm{T}} - \theta) - v_{\mathrm{M}}\sin\sigma)^2}{rv_{\mathrm{M}}\sin\sigma} - \frac{(v_{\mathrm{T}}\sin(\gamma_{\mathrm{T}} - \theta) - v_{\mathrm{M}}\sin\sigma)}{r} \\ &= \frac{1}{v_{\mathrm{M}}\sin\sigma}\left[-\frac{q(v_{\mathrm{T}}\cos(\gamma_{\mathrm{T}} - \theta) - v_{\mathrm{M}}\cos\sigma - \dot{r}_{\mathrm{d}})^{2-\frac{p}{q}}}{\beta p} + \ddot{r}_{\mathrm{d}}\right. \\ &\quad \left. - \frac{(v_{\mathrm{T}}\sin(\gamma_{\mathrm{T}} - \theta) - v_{\mathrm{M}}\sin\sigma)^2}{r}\right] - \frac{(v_{\mathrm{T}}\sin(\gamma_{\mathrm{T}} - \theta) - v_{\mathrm{M}}\sin\sigma)}{r}\end{aligned} \tag{20}$$

Our first goal is to prove that the quantity on the right-hand side of Eq. (20) does not become zero when $\sigma = 0$. Let us suppose, for the sake of contradiction, that it is zero. Then, it follows that

$$\begin{aligned}&-\frac{q(v_{\mathrm{T}}\cos(\gamma_{\mathrm{T}} - \theta) - v_{\mathrm{M}}\cos\sigma - \dot{r}_{\mathrm{d}})^{2-\frac{p}{q}}}{\beta p} + \ddot{r}_{\mathrm{d}} \\ &\quad - \frac{(v_{\mathrm{T}}\sin(\gamma_{\mathrm{T}} - \theta) - v_{\mathrm{M}}\sin\sigma)v_{\mathrm{T}}\sin(\gamma_{\mathrm{T}} - \theta)}{r} = 0\end{aligned} \tag{21}$$

Downloaded by "University of Texas, San Antonio" on June 15, 2025 | http://arc.aiaa.org | DOI: 10.2514/1.G006957

$$\Rightarrow \sin\sigma = -\left[\frac{r\ddot{r}_\mathrm{d}}{v_\mathrm{M}v_\mathrm{T}} - \frac{rq(v_\mathrm{T}\cos(\gamma_\mathrm{T}-\theta) - v_\mathrm{M}\cos\sigma - \dot{r}_\mathrm{d})^{2-\frac{p}{q}}}{\beta p v_\mathrm{M} v_\mathrm{T}} - \frac{v_\mathrm{M}}{v_\mathrm{T}}\sin^2(\gamma_\mathrm{T}-\theta)\right]\frac{1}{\sin(\gamma_\mathrm{T}-\theta)} \tag{22}$$

It can be readily verified that while the left-hand side of Eq. (22) is zero under the assumption that $\sigma = 0$, its right-hand side does not necessarily equal to zero. Thus, Eq. (22) generally does not hold, which implies that $\sigma = 0$ may not be an equilibrium point of $\dot{\sigma} = f(\sigma)$.

To further strengthen the claim that $\sigma = 0$ is not an equilibrium, we analyze the possibilities leading to the validity of Eq. (22). Using Eq. (1), the expression in Eq. (20) can be compactly written as

$$\dot{\sigma} = -\frac{(\dot{r}-\dot{r}_\mathrm{d})^{2-\frac{p}{q}}}{\beta^{\frac{p}{q}} v_\mathrm{M}\sin\sigma} + \frac{\ddot{r}_\mathrm{d}}{v_\mathrm{M}\sin\sigma} - \frac{r\dot{\theta}^2}{v_\mathrm{M}\sin\sigma} - \dot{\theta} \tag{23}$$

Assuming that Eq. (22) does hold, we have

$$\frac{1}{v_\mathrm{M}\sin\sigma}\left[-\frac{q(\dot{r}-\dot{r}_\mathrm{d})^{2-\frac{p}{q}}}{\beta p} + \ddot{r}_\mathrm{d} - r\dot{\theta}^2\right] - \dot{\theta} = 0$$

$$\Rightarrow \ddot{r}_\mathrm{d} - v_\mathrm{M}\sin\sigma\dot{\theta} - \frac{q(\dot{r}-\dot{r}_\mathrm{d})^{2-\frac{p}{q}}}{\beta p} = r\dot{\theta}^2 \tag{24}$$

which, however, is not possible, because the right-hand side of Eq. (24) is nonnegative, while the left-hand side may change sign depending on the values of $\dot{r}$, $\dot{r}_\mathrm{d}$, $\ddot{r}_\mathrm{d}$, σ, and $\dot{\theta}$. This leads to the same conclusion as obtained previously.

Now, let us separately examine whether it is at all possible for Eq. (24) to be true when $\sigma = 0$. In this case, either of the following two cases may occur:

Case I (when the pursuer is on a collision [or inverse collision] course with the target): In this case, r is decreasing (or increasing) at a fixed rate, and $\dot{\theta} = 0$. Then, no matter what value σ attains, Eq. (24) becomes

$$\ddot{r}_\mathrm{d} = \frac{q(\pm c - \dot{r}_\mathrm{d})^{2-\frac{p}{q}}}{\beta p} \tag{25}$$

where c is the constant rate at which r is increasing and $-c$ denotes the rate that r is decreasing. Now, the above quantity is zero if we intend the pursuer to hit the target (or go away from it for all time). However, target enclosing requires that r and r_d be nonzero, meaning that the above situation does not arise. Hence, we can safely exclude this scenario.

Case II [when the pursuer maintains a fixed, nonzero r_d from the target but $\dot{\theta} = 0$, namely, both sides of Eq. (24) are 0]: In this case, the pursuer is moving parallel to the target, which violates the fabric of

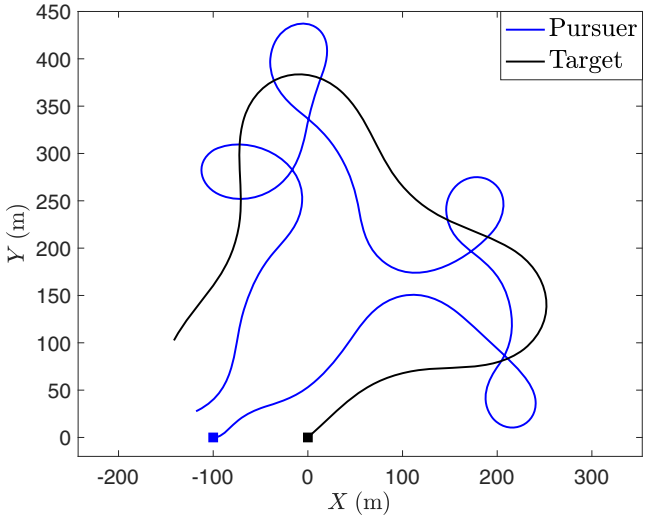

a) Trajectories

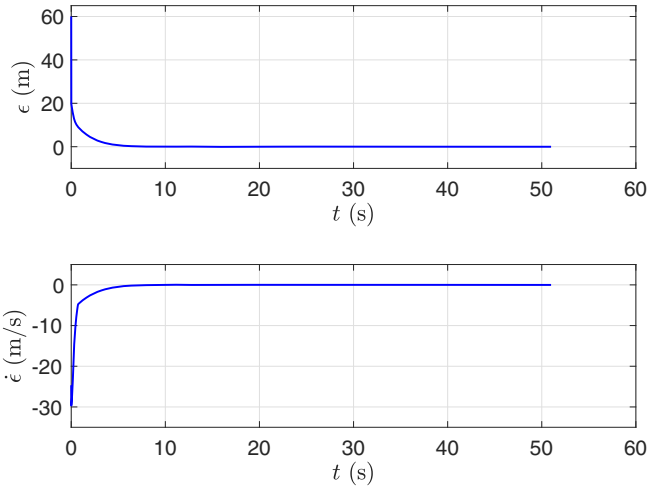

b) Error profiles

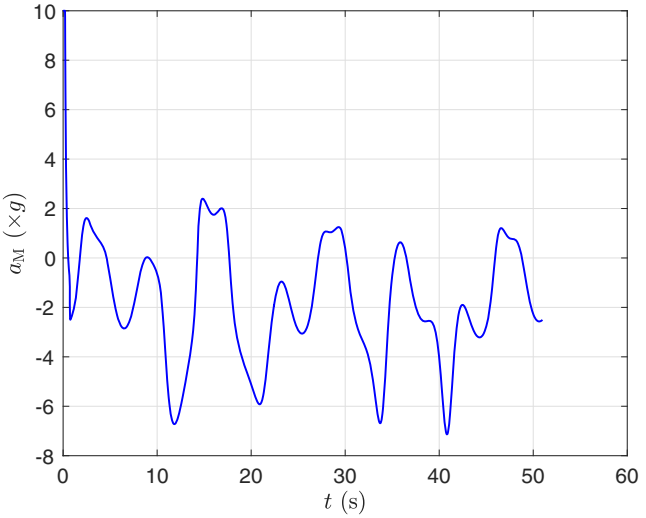

c) The pursuer's lateral acceleration

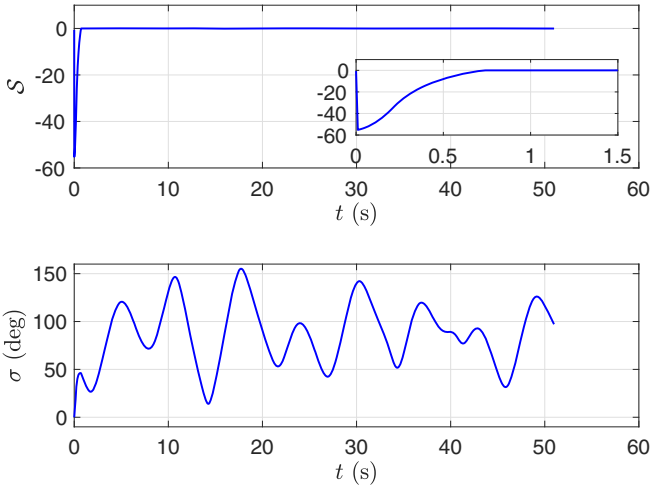

d) Sliding manifold and the pursuer's look angle

Fig. 2 Enclosing a maneuvering target within an arbitrary desired geometry.

Downloaded by "University of Texas, San Antonio" on June 15, 2025 | http://arc.aiaa.org | DOI: 10.2514/1.G006957

the target enclosing guidance. Hence, we can also disregard this scenario.

Based on the above analysis, we can conclude that $\sigma = 0$ is not an equilibrium. Hence, the proposed guidance command, Eq. (10), is nonsingular almost everywhere. This concludes the proof. □

Remark 1: Even if there exists a scenario where the pursuer's look angle becomes zero, it will not stay at that value owing to the fact that it is not an attractor, as shown in Theorem 2. In such a scenario, the pursuer will execute the maximum available lateral acceleration because the pursuer's maneuverability is always bounded in practice. As a result, the lateral acceleration demand will not shoot to an infinite value.

Remark 2: In general, the pursuer's look angle varies in accordance with the reference (or desired) target enclosing geometry. For example, the work in Refs. [24,25] designed a guidance law to make the pursuer's side-bearing angle equal to zero to enclose the target within a circle, which is equivalent to making the magnitude of the pursuer's look angle equal to $\pi/2$. In line with Theorem 2, it was shown in Refs. [30,33,34] that under certain conditions, $\sigma = 0$ implies target interception. Thus, one may speculate that cleverly shaping the pursuer's look angle may also lead to trajectories that result in target enclosing.

We now present the pursuer's lateral acceleration for enclosing a target within a circle, which is a special case of the main result proposed in this paper.

Corollary 1: Consider the planar engagement between a pursuer and a stationary target whose kinematics is governed by Eq. (1), and the error variable, Eq. (3). The pursuer's lateral acceleration

$$a_{\mathrm{M}} = \frac{-\big(\Upsilon(\mathcal{M}|\mathcal{S}|^m + \mathcal{N}|\mathcal{S}|^n)^k + \eta\big)\mathrm{sign}(\mathcal{S}) + v_{\mathrm{M}}\cos\sigma}{\beta\frac{p}{q}(-v_{\mathrm{M}}\cos\sigma)^{\frac{p}{q}-1}\sin\sigma} - \frac{v_{\mathrm{M}}^2\sin\sigma}{r} \tag{26}$$

where Υ is defined in Eq. (15), allows the pursuer to converge to a circular orbit around the target within finite time $T_s + t_c$.

Proof: For a stationary target, $v_{\mathrm{T}} = 0$ and $a_{\mathrm{T}} = 0$. Hence, upon substituting for these values in Eq. (10), one may obtain

$$a_{\mathrm{M}} = \frac{-\big(\Upsilon(\mathcal{M}|\mathcal{S}|^m + \mathcal{N}|\mathcal{S}|^n)^k + \eta\big)\mathrm{sign}(\mathcal{S}) + v_{\mathrm{M}}\cos\sigma + \dot{r}_{\mathrm{d}}}{\beta\frac{p}{q}(-v_{\mathrm{M}}\cos\sigma - \dot{r}_{\mathrm{d}})^{\frac{p}{q}-1}\sin\sigma} + \frac{r\ddot{r}_{\mathrm{d}} - v_{\mathrm{M}}^2\sin^2\sigma}{r\sin\sigma} \tag{27}$$

which is the lateral acceleration for enclosing a stationary target within an arbitrary given geometry that may not necessarily be a circle. If the given geometry is a circle, then we have $r_{\mathrm{d}}(t) = r_{\mathrm{d}}$

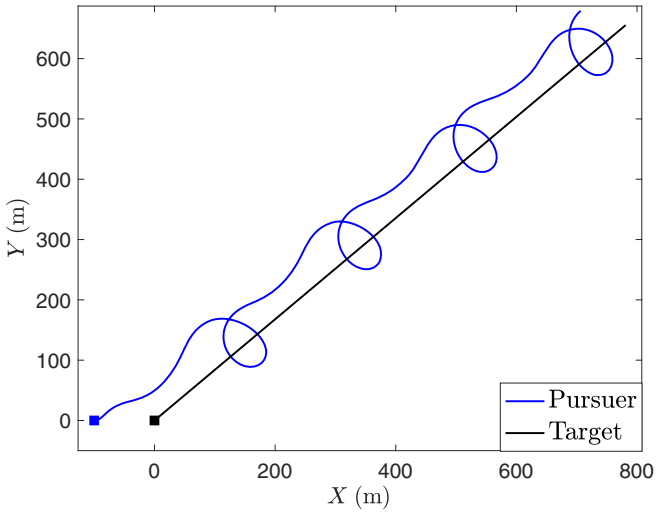

a) Trajectories

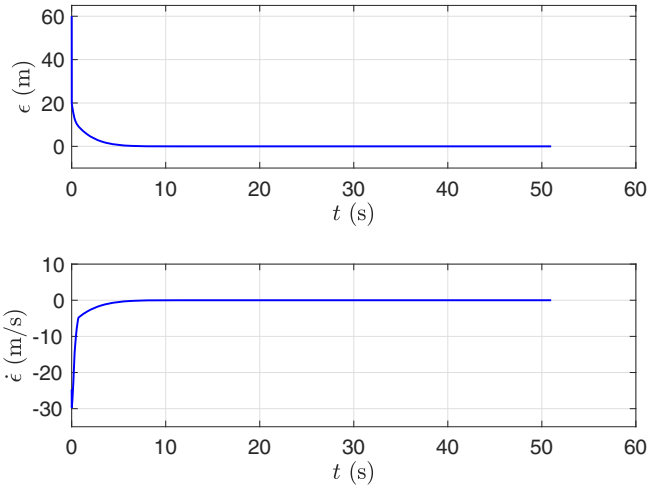

b) Error profiles

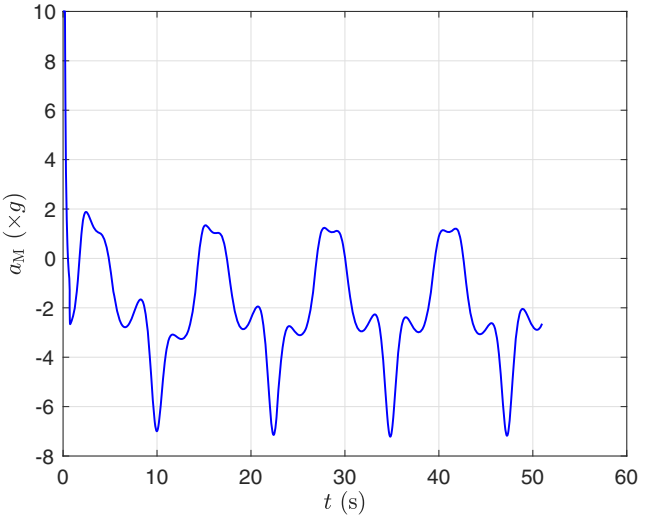

c) The pursuer's lateral acceleration

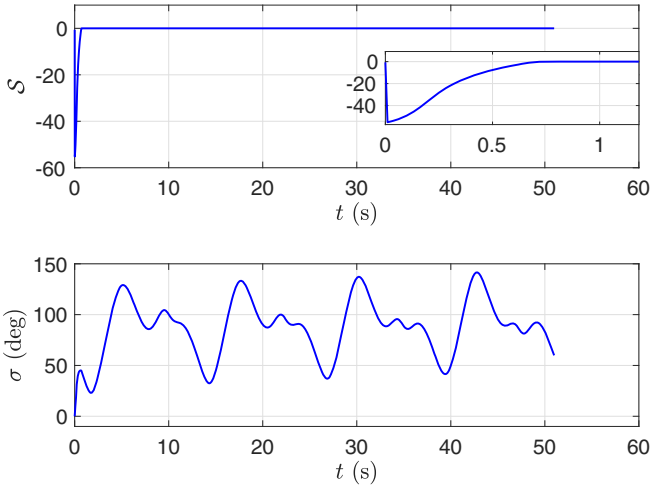

d) Sliding manifold and the pursuer's look angle

Fig. 3 Enclosing a constant-speed target within an arbitrary desired geometry.

Downloaded by "University of Texas, San Antonio" on June 15, 2025 | http://arc.aiaa.org | DOI: 10.2514/1.G006957

as a constant value, and all its subsequent derivatives are zero. Thus, Eq. (26) readily follows from Eq. (27) by letting $\dot{r}_d = \ddot{r}_d = 0$. □

Remark 3: Once sliding mode is enforced, Eq. (26) degenerates to

$$a_M = -\frac{q(-v_M \cos\sigma)^{2-\frac{p}{q}}}{\beta p \sin\sigma} - \frac{v_M^2 \sin\sigma}{r} \tag{28}$$

where the first term manipulates the pursuer's heading toward the circle until maximum value of look angle is achieved (i.e., $|\sigma| = (\pi/2)$), or its side bearing angle (as in Ref. [25]) becomes zero. Thereafter, the pursuer maintains a constant lateral acceleration; i.e.,

$$a_M = \frac{v_M^2}{r} \tag{29}$$

whose direction of encirclement depends on the initial look angle of the pursuer. For encirclement of a stationary target, it is easy to observe that $|\sigma| = (\pi/2)$ is indeed an equilibrium point of $\dot{\sigma} = f(\sigma)$, as in Theorem 2, and that $|\sigma| = (\pi/2)$ satisfies Eq. (21).

IV. Simulations

In this section, we demonstrate the efficacy of the proposed guidance strategy via simulations for a variety of scenarios.

We assume that the pursuer moves with a speed of 40 m/s while the target may either exhibit various kinds of mobility or remains stationary. Respecting the physical constraints on actuators, we limit the maximum lateral acceleration capability of the pursuer within $\pm 10g$, where g is the acceleration due to gravity. In the plots that follow, a blue square marker represents the initial position of the pursuer, whereas a black square marker is representative of the target's start position. A black circle marker appears in a plot when the target is stationary. In each case, the pursuer is initially 100 m away from the target, which is initially at the origin.

Figure 2 depicts a scenario where the target accelerates according to the law $a_T = 2 - 5\sin\left(\frac{\pi}{10}t\right)$ with a speed of 20 m/s. The target's initial heading angle is 40°, whereas the pursuer starts with a heading angle of 0°. The initial LOS angle between the vehicles is also 0°. The desired reference enclosing geometry is characterized by a time-varying relative distance, $r_d(t) = 60 + 5\sin(t) + 20\cos(t)$ with distinct upper and lower bounds. The desired reference and its subsequent derivatives are smooth and bounded, such that $r_d^{\min}(t) = 35$, $r_d^{\max}(t) = 85$, and $\dot{r}_d^{\max}(t) = \ddot{r}_d^{\max}(t) = 25$. The controller gains are chosen as $\mathcal{M} = 1, \mathcal{N} = 1, m = 0.1, n = 0.5$, and $k = 3$. The upper bound on settling time, or the upper bound on the time of convergence

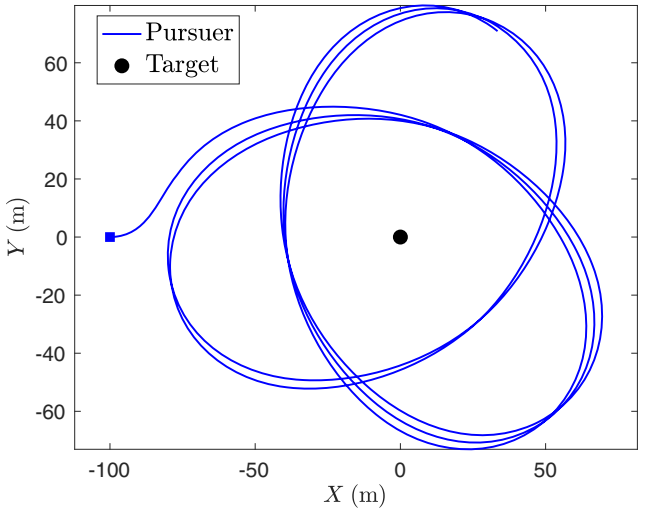

a) Trajectories

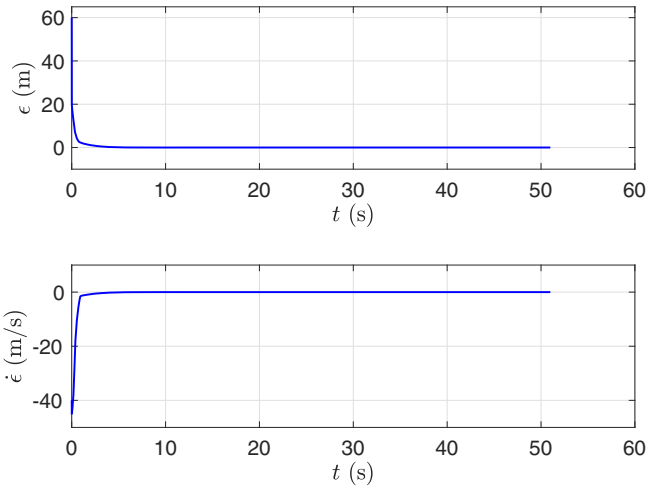

b) Error profiles

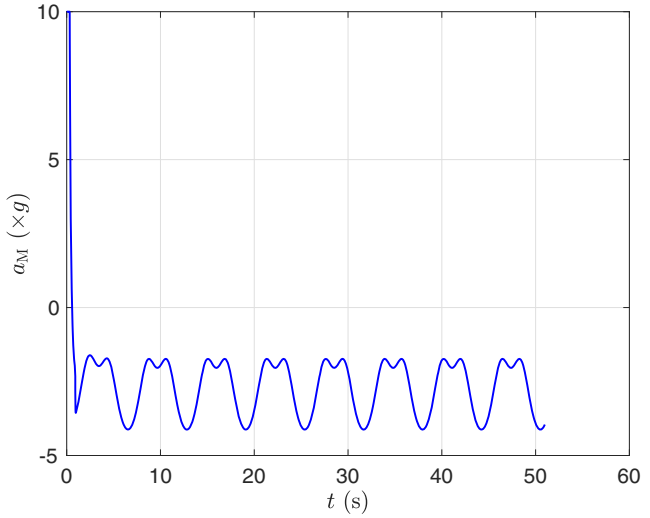

c) The pursuer's lateral acceleration

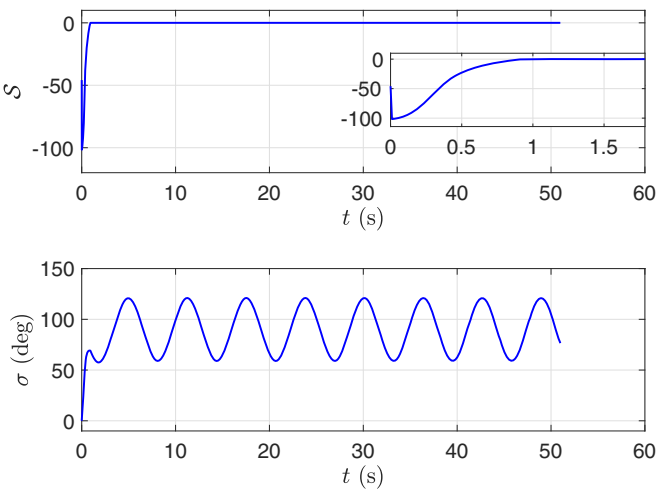

d) Sliding manifold and the pursuer's look angle

Fig. 4 Enclosing a stationary target within an arbitrary desired geometry.

Downloaded by "University of Texas, San Antonio" on June 15, 2025 | http://arc.aiaa.org | DOI: 10.2514/1.G006957

of the sliding manifold to zero, is chosen as $T_s = 3$ s. Figure 2a depicts the trajectories of the vehicles where we observe that the pursuer maneuvers in accordance with the target's motion to enclose it within the desired geometry. Because the target moves at half the speed of the pursuer, the latter makes suitable turns to go around the former as required. The error variables are shown in Fig. 2b, evidencing that they vanish quickly once the sliding mode is enforced. As observed from Fig. 2c, the lateral acceleration demand is large at the beginning, but after the occurrence of sliding mode, it decreases. It is also worth observing that, in this particular scenario, the pursuer's initial look angle is 0°, which might seem to cause a singularity in the guidance command. However, as discussed in Theorem 2, $\sigma = 0$ is only momentary as it is not an equilibrium point, leading to only a momentary increase in the lateral acceleration to its maximum value. This behavior can be observed from Fig. 2d as the look angle escapes from its zero value rapidly. Figure 2d also shows that although T_s is chosen 3 s, the sliding manifold converges to zero within 1 s, which is quite fast. This, further, allows the error variables to vanish quickly and enables the pursuer to stay on the desired geometry for all future times.

Figure 3 depicts the same scenario as that shown in Fig. 2. However, in this case, the target does not maneuver but moves at a constant speed. Under the same parameters as those in the previous case, we see that the pursuer is able to enclose the constant-speed target within the desired enclosing geometry with reasonable acceleration demand. In this scenario, the pursuer repeats its enclosing trajectory at regular intervals. This behavior is also observed in its lateral acceleration and look angle profiles.

In the scenario depicted in Fig. 4, the target is stationary. The pursuer, then, goes around the target to enclose it within the desired enclosing geometry. This particular geometry is not a circle, and it requires the pursuer to change its relative distance from the target with respect to time. Consequently, the pursuer is able to cover more regions, and this property is useful for area monitoring, surveillance, etc. Other variables of interest exhibit similar behavior as discussed previously.

Note that, in spite of circular trajectories being fuel efficient (in most cases), enclosing a target in a circle might also be prohibitive in many scenarios, e.g., when the environment is complicated or the pursuer has to accomplish a covert mission. Moreover, applications like boundary tracking, perimeter surveillance, herding/shepherding, and enclosing multiple targets naturally necessitate a guidance law capable of generating smooth enclosing patterns. Thus, the proposed guidance law is generic and has broad applicability.

To further assess the merits of the proposed design, we also let the pursuer move in a circular orbit around the target. This means that $r_{\mathrm{d}}(t)$ is a constant value, set at 40 m. For this case, the pursuer's

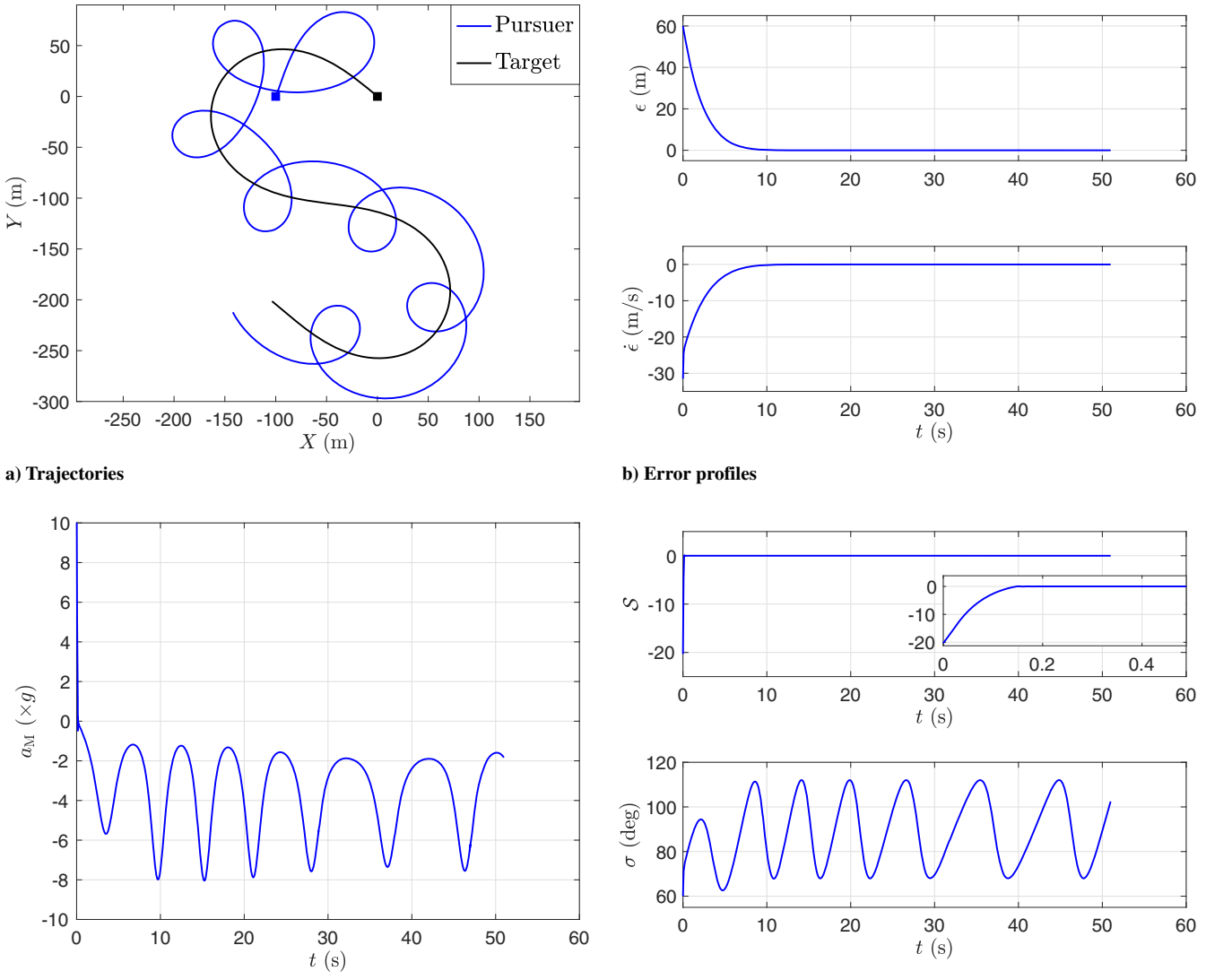

a) Trajectories **b) Error profiles**

c) The pursuer's lateral acceleration **d) Sliding manifold and the pursuer's look angle**

Fig. 5 Enclosing a maneuvering target within a circle.

Downloaded by "University of Texas, San Antonio" on June 15, 2025 | http://arc.aiaa.org | DOI: 10.2514/1.G006957

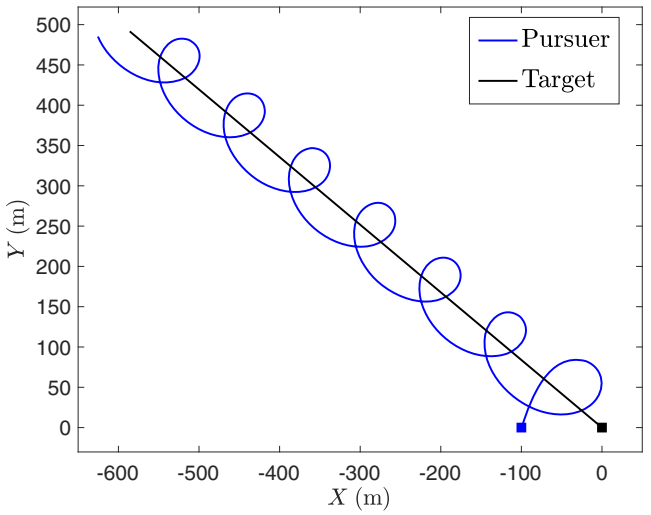

a) Trajectories

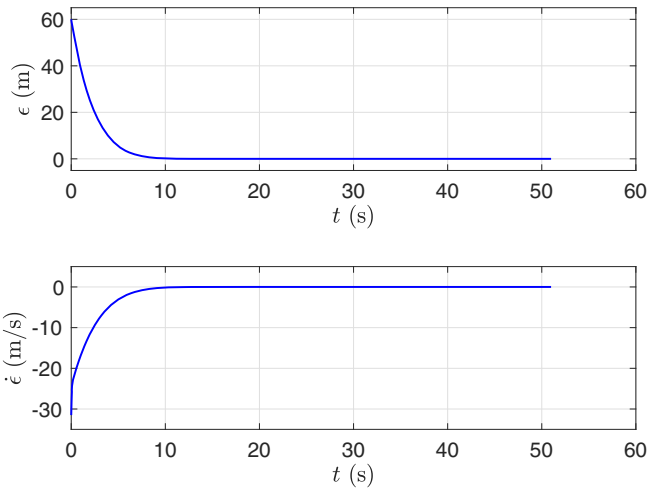

b) Error profiles

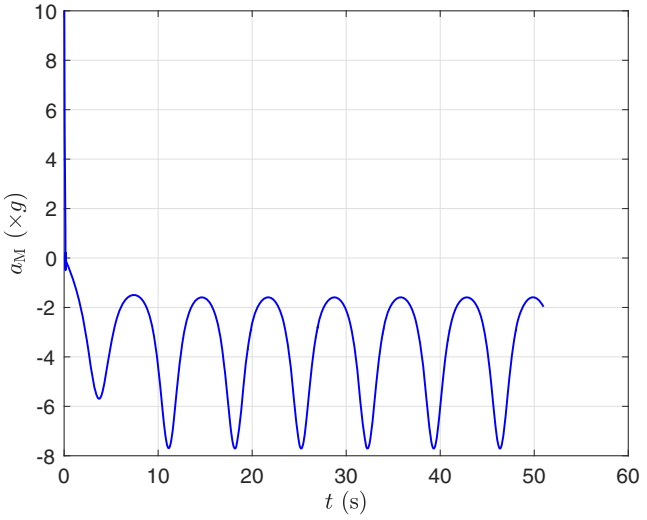

c) The pursuer's lateral acceleration

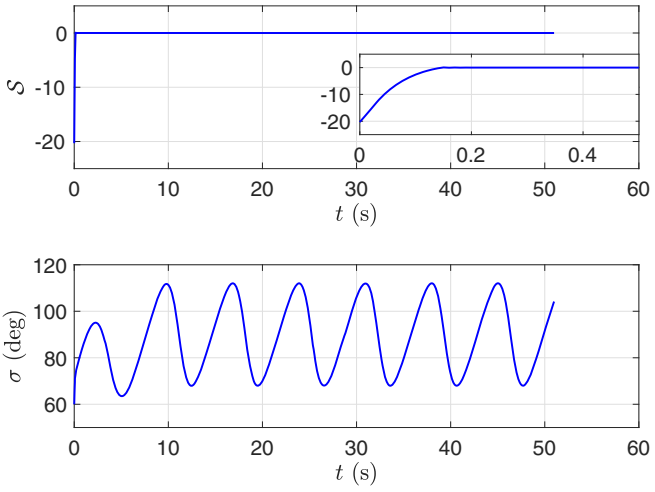

d) Sliding manifold and the pursuer's look angle

Fig. 6 Enclosing a constant-speed target within a circle.

initial heading angle is 60° and that of the target is 140°. The speed of the target is 15 m/s, while it maneuvers according to $a_T = 3.5\sin((\pi/25)t)$, as shown in Fig. 5. The initial LOS angle is 0°. The controller parameters for this and the next cases are chosen as $\mathcal{M} = 3$, $\mathcal{N} = 1$, $m = 0.15$, $n = 1.01$, and $k = 1.01$. It is easy to verify that the gains satisfy the criterion in Lemma 2. As seen in Fig. 5, the lateral acceleration demand is high in the transient phase. This is because the pursuer needs more control effort in the beginning to reach the desired enclosing geometry. It is also worth noting that the lateral acceleration does not hit saturation limits as the look angle never becomes zero. While $T_s = 4$ s in this case, the sliding manifold converges to zero within 0.5 s. This quick convergence allows the error variables to settle down to zero soon after sliding mode is enforced.

If the target does not maneuver, then the pursuer follows a spiral/helical resembling path to enclose the constant-speed target, as seen from Fig. 6. Because the design parameters are kept the same as that in the previous case, the error profiles show a similar trend in this case as well. As discussed earlier, the pursuer now periodically encloses the constant-speed target. Thus, the profiles of lateral acceleration and the look angle are also periodic in the steady state.

Finally, we also demonstrate the most celebrated scenario when it comes to target enclosing—encirclement of a stationary target, or a circumnavigation. Figure 7 illustrates that the pursuer goes in a circle of a fixed radius around a stationary target. The pursuer's guidance command for this case is given by Eq. (26), as in Corollary 1. Note that encirclement is a special case of target enclosing where the pursuer's lateral acceleration becomes constant, and the magnitude of its look angle rises to a maximum ($|\sigma| = \pi/2$).

V. Conclusions

In this work, we presented a novel guidance strategy to enclose a general maneuvering target within any smooth and bounded geometrical shape. Our work generalizes the existing target enclosing guidance strategies originally designed for target encirclement. By considering the lateral acceleration of the pursuer as its steering control, our design accounts for the inherent constraints on the pursuer's heading and turn rate. Our design was based on predefined-time convergent sliding mode control. Thus, the proposed design has the flexibility to tailor the duration of the transient phase by specifying the upper bound on the settling time directly in the guidance command. In essence, the convergence of the sliding manifold to zero can be dictated through the guidance command, which was independent of the initial engagement conditions. The proposed guidance command relied on relative information only and did not require the target's guidance law during design, thereby making the design simple. Enclosing a mobile target in three dimensions and incorporating multi-agent collective motions may be of interest in future investigations. Moreover, an optimal enclosing

Downloaded by "University of Texas, San Antonio" on June 15, 2025 | http://arc.aiaa.org | DOI: 10.2514/1.G006957

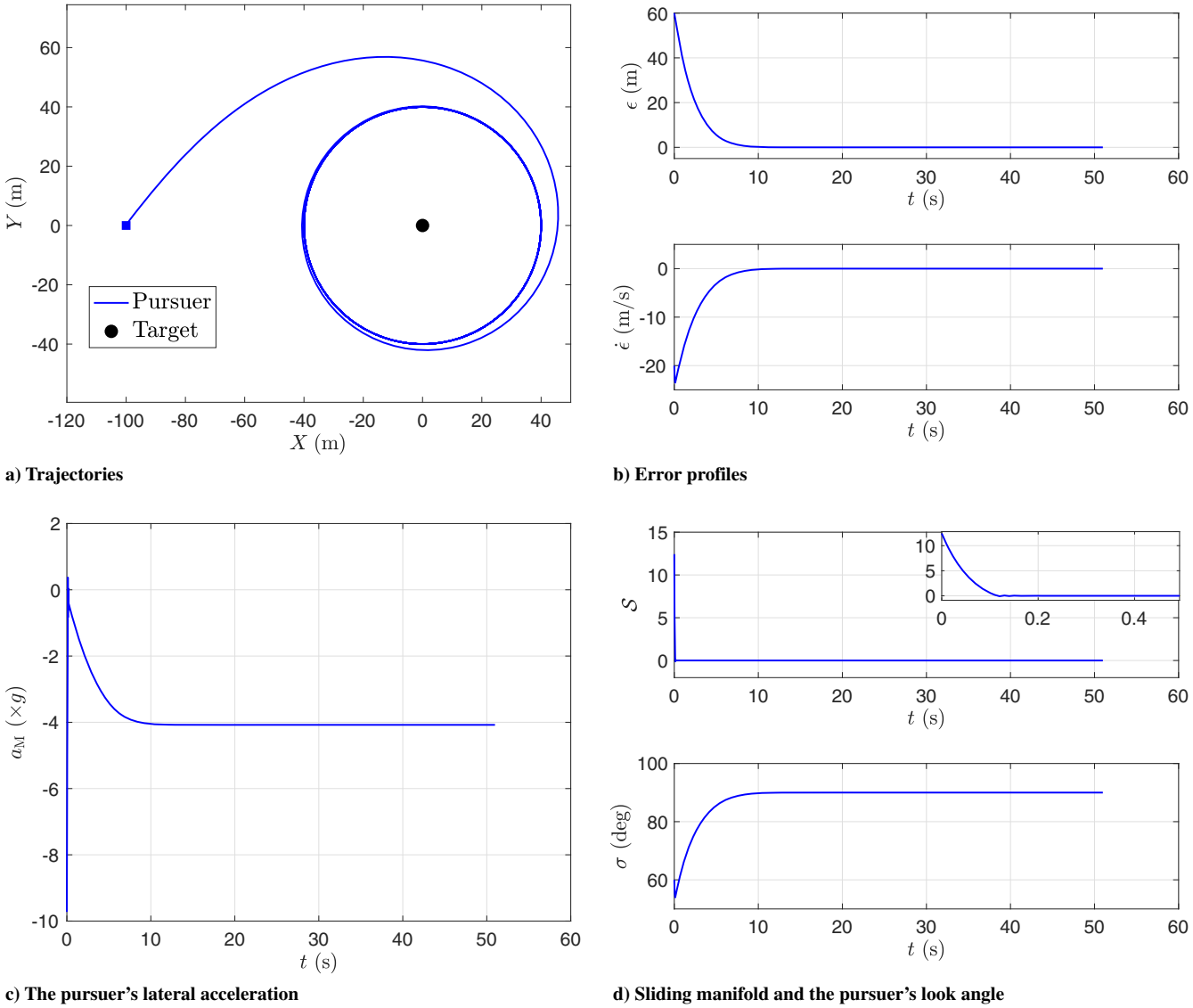

a) Trajectories **b) Error profiles**

c) The pursuer's lateral acceleration **d) Sliding manifold and the pursuer's look angle**

Fig. 7 Enclosing a stationary target within a circle of radius 40 m.

behavior in the presence of obstacles could also be an interesting research topic.

Acknowledgment

This work was supported by the Office of Naval Research under Grant N00014-19-1-2278.

References

[1] Yamaguchi, H., "A Cooperative Hunting Behavior by Mobile-Robot Troops," *International Journal of Robotics Research*, Vol. 18, No. 9, 1999, pp. 931–940. https://doi.org/10.1177/02783649922066664

[2] Kim, T.-H., and Sugie, T., "Cooperative Control for Target-Capturing Task Based on a Cyclic Pursuit Strategy," *Automatica*, Vol. 43, No. 8, 2007, pp. 1426–1431. https://doi.org/10.1016/j.automatica.2007.01.018

[3] Guo, J., Yan, G., and Lin, Z., "Local Control Strategy for Moving-Target-Enclosing Under Dynamically Changing Network Topology," *Systems & Control Letters*, Vol. 59, No. 10, 2010, pp. 654–661. https://doi.org/10.1016/j.sysconle.2010.07.010

[4] Zheng, R., and Sun, D., "Rendezvous of Unicycles: A Bearings-Only and Perimeter Shortening Approach," *Systems & Control Letters*, Vol. 62, No. 5, 2013, pp. 401–407. https://doi.org/10.1016/j.sysconle.2013.02.006

[5] Ceccarelli, N., Di Marco, M., Garulli, A., and Giannitrapani, A., "Collective Circular Motion of Multi-Vehicle Systems," *Automatica*, Vol. 44, No. 12, 2008, pp. 3025–3035. https://doi.org/10.1016/j.automatica.2008.04.024

[6] Lan, Y., Yan, G., and Lin, Z., "Distributed Control of Cooperative Target Enclosing Based on Reachability and Invariance Analysis," *Systems & Control Letters*, Vol. 59, No. 7, 2010, pp. 381–389. https://doi.org/10.1016/j.sysconle.2010.04.003

[7] Lu, P., Lewis, A., Adams, R. J., DeVore, M. D., and Petersen, C. D., "Finite-Thrust Natural-Motion Circumnavigation Injection by Convex Optimization," *Journal of Guidance, Control, and Dynamics*, Vol. 45, No. 3, 2022, pp. 453–467. https://doi.org/10.2514/1.G006123

[8] Kokolakis, N.-M. T., and Koussoulas, N. T., "Robust Standoff Target Tracking with Finite-Time Phase Separation Under Unknown Wind," *Journal of Guidance, Control, and Dynamics*, Vol. 44, No. 6, 2021, pp. 1183–1198. https://doi.org/10.2514/1.G005517

[9] Frew, E. W., Lawrence, D. A., and Morris, S., "Coordinated Standoff Tracking of Moving Targets Using Lyapunov Guidance Vector Fields," *Journal of Guidance, Control, and Dynamics*, Vol. 31, No. 2, 2008, pp. 290–306. https://doi.org/10.2514/1.30507

[10] Summers, T. H., Akella, M. R., and Mears, M. J., "Coordinated Standoff Tracking of Moving Targets: Control Laws and Information Architectures," *Journal of Guidance, Control, and Dynamics*, Vol. 32, No. 1, 2009, pp. 56–69. https://doi.org/10.2514/1.37212

Downloaded by "University of Texas, San Antonio" on June 15, 2025 | http://arc.aiaa.org | DOI: 10.2514/1.G006957

[11] Lim, S., Kim, Y., Lee, D., and Bang, H., "Standoff Target Tracking Using a Vector Field for Multiple Unmanned Aircrafts," *Journal of Intelligent & Robotic Systems*, Vol. 69, Jan. 2013, pp. 347–360. https://doi.org/10.1007/s10846-012-9765-7

[12] Pothen, A. A., and Ratnoo, A., "Curvature-Constrained Lyapunov Vector Field for Standoff Target Tracking," *Journal of Guidance, Control, and Dynamics*, Vol. 40, No. 10, 2017, pp. 2729–2736. https://doi.org/10.2514/1.G002281

[13] Quigley, M., Goodrich, M., Griffiths, S., Eldredge, A., and Beard, R., "Target Acquisition, Localization, and Surveillance Using a Fixed-Wing Mini-UAV and Gimbaled Camera," *Proceedings of the 2005 IEEE International Conference on Robotics and Automation*, 2005, pp. 2600–2605. https://doi.org/10.1109/ROBOT.2005.1570505

[14] Chen, H., Chang, K., and Agate, C. S., "Tracking with UAV Using Tangent-Plus-Lyapunov Vector Field Guidance," *2009 12th International Conference on Information Fusion*, 2009, pp. 363–372.

[15] Kim, S., Oh, H., and Tsourdos, A., "Nonlinear Model Predictive Coordinated Standoff Tracking of a Moving Ground Vehicle," *Journal of Guidance, Control, and Dynamics*, Vol. 36, No. 2, 2013, pp. 557–566. https://doi.org/10.2514/1.56254

[16] Yoon, S., Park, S., and Kim, Y., "Circular Motion Guidance Law for Coordinated Standoff Tracking of a Moving Target," *IEEE Transactions on Aerospace and Electronic Systems*, Vol. 49, No. 4, 2013, pp. 2440–2462. https://doi.org/10.1109/TAES.2013.6621827

[17] Shames, I., Dasgupta, S., Fidan, B., and Anderson, B. D. O., "Circumnavigation Using Distance Measurements Under Slow Drift," *IEEE Transactions on Automatic Control*, Vol. 57, No. 4, 2012, pp. 889–903. https://doi.org/10.1109/TAC.2011.2173417

[18] Matveev, A. S., Teimoori, H., and Savkin, A. V., "Range-Only Measurements Based Target Following for Wheeled Mobile Robots," *Automatica*, Vol. 47, No. 1, 2011, pp. 177–184. https://doi.org/10.1016/j.automatica.2010.10.025

[19] Cao, Y., "UAV Circumnavigating an Unknown Target Under a GPS-Denied Environment with Range-Only Measurements," *Automatica*, Vol. 55, May 2015, pp. 150–158. https://doi.org/10.1016/j.automatica.2015.03.007

[20] Dong, F., You, K., and Song, S., "Target Encirclement with any Smooth Pattern Using Range-Based Measurements," *Automatica*, Vol. 116, June 2020, Paper 108932. https://doi.org/10.1016/j.automatica.2020.108932

[21] Deghat, M., Shames, I., Anderson, B. D. O., and Yu, C., "Localization and Circumnavigation of a Slowly Moving Target Using Bearing Measurements," *IEEE Transactions on Automatic Control*, Vol. 59, No. 8, 2014, pp. 2182–2188. https://doi.org/10.1109/TAC.2014.2299011

[22] Zheng, R., Liu, Y., and Sun, D., "Enclosing a Target by Nonholonomic Mobile Robots with Bearing-Only Measurements," *Automatica*, Vol. 53, 2015, pp. 400–407. https://doi.org/10.1016/j.automatica.2015.01.014

[23] Jain, P., and Peterson, C. K., "Encirclement of Moving Targets Using Relative Range and Bearing Measurements," *2019 International Conference on Unmanned Aircraft Systems (ICUAS)*, IEEE Publ., Piscataway, NJ, 2019, pp. 43–50. https://doi.org/10.1109/ICUAS.2019.8798252

[24] Park, S., "Circling over a Target with Relative Side Bearing," *Journal of Guidance, Control, and Dynamics*, Vol. 39, No. 6, 2016, pp. 1454–1458. https://doi.org/10.2514/1.G001421

[25] Park, S., "Guidance Law for Standoff Tracking of a Moving Object," *Journal of Guidance, Control, and Dynamics*, Vol. 40, No. 11, 2017, pp. 2948–2955. https://doi.org/10.2514/1.G002707

[26] Aldana-López, R., Gómez-Gutiérrez, D., Jiménez-Rodríguez, E., Sánchez-Torres, J. D., and Defoort, M., "Enhancing the Settling Time Estimation of a Class of Fixed-Time Stable Systems," *International Journal of Robust and Nonlinear Control*, Vol. 29, No. 12, 2019, pp. 4135–4148. https://doi.org/10.1002/rnc.4600

[27] Sinha, A., Kumar, S. R., and Mukherjee, D., "Nonsingular Impact Time Guidance and Control Using Deviated Pursuit," *Aerospace Science and Technology*, Vol. 115, Aug. 2021, Paper 106776. https://doi.org/10.1016/j.ast.2021.106776

[28] Sinha, A., Kumar, S. R., and Mukherjee, D., "Cooperative Salvo Based Active Aircraft Defense Using Impact Time Guidance," *IEEE Control Systems Letters*, Vol. 5, No. 5, 2021, pp. 1573–1578. https://doi.org/10.1109/LCSYS.2020.3041799

[29] Idan, M., Shima, T., and Golan, O. M., "Integrated Sliding Mode Autopilot-Guidance for Dual-Control Missiles," *Journal of Guidance, Control, and Dynamics*, Vol. 30, No. 4, 2007, pp. 1081–1089. https://doi.org/10.2514/1.24953

[30] Tsalik, R., and Shima, T., "Circular Impact-Time Guidance," *Journal of Guidance, Control, and Dynamics*, Vol. 42, No. 8, 2019, pp. 1836–1847. https://doi.org/10.2514/1.G004074

[31] Sinha, A., Kumar, S. R., and Mukherjee, D., "Impact Time Constrained Integrated Guidance and Control Design," *Aerospace Science and Technology*, Vol. 115, Aug. 2021, Paper 106824. https://doi.org/10.1016/j.ast.2021.106824

[32] Sinha, A., Kumar, S. R., and Mukherjee, D., "Three-Agent Time-Constrained Cooperative Pursuit-Evasion," *Journal of Intelligent & Robotic Systems*, Vol. 104, No. 28, 2022, pp. 1–27. https://doi.org/10.1007/s10846-022-01570-y

[33] Sinha, A., Kumar, S. R., and Mukherjee, D., "Three-Dimensional Nonlinear Cooperative Salvo Using Event-Triggered Strategy," *Journal of Guidance, Control, and Dynamics*, Vol. 44, No. 2, 2021, pp. 328–342. https://doi.org/10.2514/1.G005367

[34] Sinha, A., Kumar, S. R., and Mukherjee, D., "Three-Dimensional Guidance with Terminal Time Constraints for Wide Launch Envelops," *Journal of Guidance, Control, and Dynamics*, Vol. 44, No. 2, 2021, pp. 343–359. https://doi.org/10.2514/1.G005180

Downloaded by "University of Texas, San Antonio" on June 15, 2025 | http://arc.aiaa.org | DOI: 10.2514/1.G006957